

Integrating Spectral, Spatial, and Terrain Variables for Forest Ecosystem Classification

Paul Treitz and Philip Howarth

Abstract

Sets of spectral, spectral-spatial, textural, and geomorphometric variables derived from high spatial resolution Compact Airborne Spectrographic Imager (CASI) and elevation data are tested to determine their ability to discriminate landscape-scale forest ecosystem classes for a study area in northern Ontario, Canada. First, linear discriminant analysis for various spectral and spectral-spatial variables indicated that a spatial resolution of approximately 6 m was optimal for discriminating six landscape-scale forest ecosystem classes. Second, texture features, using second-order spatial statistics, significantly improved discrimination of the classes over the original reflectance data. Finally, addition of terrain descriptors improved discrimination of the six forest ecosystem classes. It has been demonstrated that, in a low- to moderate-relief boreal environment, addition of textural and terrain variables to high-resolution CASI reflectance data provides improved discrimination of forest ecosystem classes.

Introduction

In an ecosystem approach to land classification, coherent terrain units may be defined by a complex of factors including vegetation, landforms, and drainage. Because forest ecosystems in northwestern Ontario, Canada are defined, in part, by physiography, it seems logical that incorporation of terrain variables with remote sensing data would improve mapping of forest ecosystems at landscape scales. It has been demonstrated that geomorphometric variables (e.g., elevation, gradient) provide additional information for discriminating land-cover classes in combination with satellite remote sensing data in high-relief environments (e.g., Frank, 1988; Peddle and Franklin, 1991; Franklin *et al.*, 1994; Michaelsen *et al.*, 1994; Florinsky and Kuryakova, 1996; Gong *et al.*, 1996; Ekstrand, 1996; Florinsky, 1998; Vogelmann *et al.*, 1998). However, it is not clear whether these terrain variables contribute additional information for discriminating forest ecosystem classes in a low- to moderate-relief boreal environment when combined with high-resolution remote sensing data.

The Forest Ecosystem Classification (FEC) for northwestern Ontario represents an ecologically based classification which incorporates physiographic and biotic elements of the forest ecosystem (Sims *et al.*, 1989). The FEC framework incorporates

those components of forest site that contribute to forest development (i.e., canopy and understory vegetation, soils, landform, general climatic regime, and regional physiography) (Sims and Uhlig, 1992). FECs were developed for stand-level (i.e., < 10 hectares) application to provide information regarding vegetation, soil, and site conditions. However, this detailed ecosystem classification is difficult to implement for large tracts of boreal forest that are characteristic of much of northwestern Ontario, Canada. Because the FEC framework is somewhat hierarchical, field-level units can be aggregated to create coarser resolution ecosystem units based on moisture and nutrient regimes (Racey *et al.*, 1989). Essentially, a range of forest ecosystem classes can be derived that account for a range of scales of application, thereby creating an ecosystem classification that is "mappable" using spectral and terrain variables, also acquired at a range of scales. Thus, integration of appropriately "scaled" and spatially processed georeferenced remote sensing data and spatially geocoded terrain information offers potential for assisting in the analysis of large areas of forest for identification of relevant landscape-scale ecosystem classes, particularly within the context of a hierarchical classification scheme.

In digital image classification of remote sensing data, decision rules based on spectral reflectance or radiance of landscape elements are applied to image data to define ecological units. It may be appropriate to incorporate terrain attributes (e.g., elevation, gradient, local relief) into the statistical decision rules to classify ecological units using remote sensing data (Moore *et al.*, 1991). At landscape scales, the primary causes which determine the differences between ecosystem units are topographic position, parent material, and slope, aspect, and inclination with controlling factors being moisture regime, soil fertility, microclimate, and snow depth (Hills and Pierpoint, 1960). At the stand level, these causes and controlling factors are important along with disturbance history (Damman, 1979). It therefore seems reasonable to expect digital terrain descriptors (e.g., elevation, gradient, aspect) to assist in the discrimination of landscape-scale forest ecosystem classes when integrated with spectral data (Florinsky and Kuryakova, 1996; Florinsky, 1998).

Texture, or the intrinsic spatial variability of tone, is recognized as an important interpretive tool for discriminating different land-cover and land-use types and is a function of spatial resolution or scale. This concept is dependent on three variables: (1) size of the area being investigated/processed, (2) the relative sizes of the discrete tonal features, and (3) spatial distribution of discrete tonal features (Baraldi and Parmiggiani,

P. Treitz was with the Department of Geography, Faculty of Arts, and Faculty of Environmental Studies, York University, 4700 Keele Street, North York, Ontario M3J 1P3, Canada. He is presently with the Department of Geography, Faculty of Arts and Science, Queen's University, Kingston, Ontario K7L 3N6, Canada (pt6@silver.queensu.ca).

P. Howarth is with the Department of Geography, Faculty of Environmental Studies, University of Waterloo, Waterloo, Ontario N2L 3G1, Canada (howarth@watleo.uwaterloo.ca).

Photogrammetric Engineering & Remote Sensing
Vol. 66, No. 3, March 2000, pp. 305-317.

0099-1112/00/6603-305\$3.00/0

© 2000 American Society for Photogrammetry
and Remote Sensing

1995). A texture field within an image is described as homogeneous if the spatial arrangement of pixel values are more homogeneous (as a unit) within than between texture fields (Barber *et al.*, 1993). It has been demonstrated that texture transforms have a role in image analysis for forestry by improving the accuracy of the interpretation of forest types and conditions (Wilson, 1996; Cain *et al.*, 1997; Wulder *et al.*, 1998). For instance, stand structural characteristics (e.g., diameter at breast height (dbh), crown diameter, density, basal area, and age) have been found to be highly correlated with texture images generated from SPOT panchromatic data (Cohen and Spies, 1992). Texture also appears to be more evident at high spatial resolutions (e.g., <10 m) as stand structural characteristics tend to, at these levels, dominate the scene (Yuan *et al.*, 1991; Franklin and McDermid, 1993). Ecologists are also examining these texture measures for development as "pattern indices" for ecological data sets (Musick and Grover, 1990; Cain *et al.*, 1997). In this study, the gray-level co-occurrence matrix (GLCM) statistical method is used to generate texture features from Compact Airborne Spectrographic Imager (CASI) data.

It has been proposed that landscape-scale site classification can provide the basis for detailed applications and planning, especially when spatial analysis and modeling techniques are applied using remote sensing and other spatial data in conjunction with field-oriented classifications (Sims *et al.*, 1994). It is recognized that many ecological and timber resources cannot be directly sensed using remotely sensed data, but must be modeled or derived from other sources of primary data. This is a natural conclusion based on a holistic ecosystem concept. The approach taken in this study is to collect high-resolution remote sensing data, derive appropriately scaled and processed images for different forest ecosystems, and integrate these features with terrain descriptors derived for landscape-scale analysis. It is suggested that, by deriving optimal spectral, textural, and terrain descriptors of the vegetation and landscape, discrimination of landscape-scale forest ecosystems can be optimized.

The objective of this study is to determine the extent to which texture and terrain variables can improve forest ecosystem mapping within the boreal forest of northwestern Ontario. An integrated dataset is developed to model forest ecosystems that incorporates multi-spatial resolution remote sensing data, texture variables, and terrain variables. High-resolution CASI data are spatially averaged to generate "optimally" and variously scaled remote sensing data. CASI spectral and spatial variables are used in combination with texture variables (mean, contrast, and correlation) and geomorphometric variables (elevation, local relief, gradient) to test the discriminability of forest ecosystems at a landscape scale (1:20,000).

Study Area Description

The study site is located approximately 100 km north of Thunder Bay, Ontario within the Central Plateau section of the Boreal Forest Region (Rowe, 1972). The area consists of a diverse mosaic of forest-stand types with various soil and landform conditions, primarily of glacial origin. Trembling aspen (*Populus tremuloides* Michx.) and black spruce (*Picea mariana* (Mill.) BSP.) are dominant with jack pine (*Pinus banksiana* Lamb.), white spruce (*Picea glauca* (Moench) A. Voss), balsam fir (*Abies balsamea* (L.) Mill.), white birch (*Betula papyrifera* Marsh.), white cedar (*Thuja occidentalis* L.), and tamarack (*Larix laricina* (Du Roi) K. Koch) occurring in various mixtures. Forest-stand overstories are monospecific or mixed, and understories range from shrub- and/or herb-rich to poor (Walsh *et al.*, 1994). The FEC applicable to the study area is the Northwestern Ontario FEC (Sims *et al.*, 1989). The ecosystem units derived from the NWO FEC for the Rinker Lake area and used in this study are listed in Table 1.

The physiography of the study site is bedrock-controlled

TABLE 1. FEC VEGETATION TYPES (V-TYPES) FOR THE RINKER LAKE STUDY AREA

V-Type*	FEC Description
Aspen-Dominated	Hardwood and Mixedwood
V5	Aspen Hardwood
V6	Trembling Aspen (White Birch)—Balsam Fir/ Mountain Maple
V7	Trembling Aspen—Balsam Fir/Balsam Fir Shrub
V8	Trembling Aspen (White Birch)/Mountain Maple
V9	Trembling Aspen Mixedwood
V10	Trembling Aspen—Black Spruce—Jack Pine/Low Shrub
White Spruce/Balsam Fir Conifer and Mixedwood	
V14	Balsam Fir Mixedwood
V15	White Spruce Mixedwood
V16	Balsam Fir—White Spruce Mixedwood/ Feathermoss
V24	White Spruce—Balsam Fir/Shrub Rich
V25	White Spruce—Balsam Fir/Feathermoss
Cedar Mixedwood	
V22	Cedar (inc. Mixedwood)/Speckled Alder/ Sphagnum
Upland Black Spruce/Jack Pine	
V31	Black spruce—Jack Pine/Tall Shrub/ Feathermoss
V32	Jack Pine—Black Spruce/Ericaceous Shrub/ Feathermoss
V33	Black Spruce/Feathermoss
Lowland Black Spruce	
V34	Black Spruce/Labrador Tea/Feathermoss (Sphagnum)
V35	Black Spruce/Speckled Alder/Sphagnum
V36	Black Spruce/Bunchberry/Sphagnum (Feathermoss)
V37	Black Spruce/Ericaceous Shrub/Sphagnum
Wetland Black Spruce	
V38	Black Spruce/Leatherleaf/Sphagnum

*Sims *et al.*, (1989)

with elevations ranging from 430 m to 530 m. The study site lies within the Severn Upland physiographic unit, in the James Bay Region of the Precambrian Shield (Mollard and Mollard, 1981). The glacial deposits in the area originate from the Wisconsinan glaciation. The predominant ice flow was from the northeast to southwest. Glacial drift is generally less than 3 m with till being the oldest and most widespread sediment in the area. This till consists of a predominantly sand to silty-sand matrix with a coarse fragment content ranging from less than 5 percent to greater than 30 percent (by volume) (Walsh *et al.*, 1994). The glaciofluvial deposits of eskers, crevasse fills, kames, and kame terraces have moderately well- to well-sorted sand and gravelly sand textures. Mineral soils in the area are moderately deep (60 to 100 cm) to deep (>100 cm), with significant amounts of coarse fragments, while very thin soils (< 20 cm), exposed bedrock, and organic soils occur to a lesser extent throughout the study area (Walsh *et al.*, 1994).

Data Description

Ground Data Collection

Ground data were collected using a methodology devised by Forestry Canada for characterizing Vegetation Types (V-Types) within a forest stand (McLean and Uhlig, 1987). FEC plots are 10- by 10-m quadrats where V-Types are determined based on the presence and abundance of canopy and secondary trees; high, low, and dwarf shrubs; broadleaf herbs; and mosses and

lichens. Here, detailed FEC plot data were collected for 71 forested sites within the study area during the periods 21 June to 15 July 1993 and 04 to 15 July 1994. Data collected for each 10- by 10-m sample plot included (1) differential Global Positioning System (GPS) data, (2) vegetation data (species and percent cover for tree, shrub, and herb layers), (3) mensuration data (age, height, density, diameter breast height (dbh)), and (4) canopy data (visual estimates of mean maximum crown diameter (MMCD)). Percent cover for each species was determined by visual estimation of (1) dominant, main canopy, and secondary trees; (2) high, low, and dwarf shrubs; (3) broadleaf herbs; and (4) mosses and lichens. In total, plot data were collected for 25 of the 38 V-Types within the NWO FEC. Of the 13 V-Types not sampled, six of these were characteristics of the Great Lakes - St. Lawrence forest to the south of the study site, four were too small in extent to be sampled effectively, and three did not occur within the study site (Kalnins *et al.*, 1994). In 1994 and 1995, a series of transects was traversed through selected forest stands in order to collect additional V-Type data. These samples of V-Type characterization only, occurred at fixed intervals of 50 m along predetermined transects.

Compact Airborne Spectrographic Imager (Reflectance) Data

The CASI is a visible/near-infrared pushbroom imaging spectrograph with a reflection grating and a two-dimensional CCD solid-state array measuring 512 by 288 pixels. The specifications of the CASI are outlined in Table 2.

CASI data were acquired from a Piper Navajo Chieftan aircraft on 30 July 1993 at an altitude of 2630 m above ground level (AGL) (Kalnins *et al.*, 1994). To minimize bidirectional reflectance (BRF) and effectively cover the study area, flight lines were oriented parallel to the solar azimuth (i.e., away from the sun), restricting data collection to a two-hour time window (10:30 a.m. to 12:30 p.m. local time). Flight lines were flown over the study site at a ground speed of 149 knots (76.7 meters/second) heading 300 degrees true with the sensor pointing at nadir. This provided an integration time of 70 milliseconds. The CASI data were collected in nine spectral bands (Table 3) and possessed a spatial resolution of 3.18 m in the cross-track direction and 5.36 m in the along-track direction.

CASI data were converted to radiance using software developed at the Center for Research in Earth and Space Technologies (CRESTech) and the algorithms of Baby and Soffer (1992). This conversion was applied in order to eliminate artifacts present in the imagery and to convert digital numbers from arbitrary values to physical units of radiance (Shepherd, 1994). The data were then converted to reflectance to eliminate atmospheric

TABLE 2. DESCRIPTION OF THE COMPACT AIRBORNE SPECTROGRAPHIC IMAGER (CASI) (ADAPTED FROM GOWER *ET AL.* (1992)).

Parameter	Description
Spectral Coverage	418 nm to 926 nm using 288 detectors; sampling interval 1.8 nm; spectral resolution 2.9 nm
Spectral Mode	39 spectra of the full 418 nm to 926 nm range are recorded, with 2.9 nm resolution, from 39 different directions across the swath; a full-resolution image at a predetermined wavelength is also recorded to assist in track recovery
Spatial Coverage	35.5° swath, with standard lens; single camera gives 612 pixels; sampling interval 1.2 mrad; spatial resolution 1.6 mrad
Spatial Mode	spectral pixels are grouped to form up to 15 bands (512 pixels wide); band width and spectral position are under software control; the number of bands governs the integration time

TABLE 3. CASI IMAGING MODE WAVELENGTHS

Feature Number	Center Wavelength (nm)	Bandwidth (nm)	Band Range (nm)
1	450.31	31.18	434.72-465.90
2	549.47	20.80	539.07-559.87
3	590.50	20.88	580.06-600.94
4	633.48	20.94	623.01-643.95
5	670.30	15.60	662.50-678.10
6	739.72	10.22	734.61-744.83
7	746.95	6.62	743.64-750.26
8	790.38	10.24	785.26-795.50
9	873.85	28.44	859.63-888.07

effects and compensate for changes in solar illumination during image acquisition. Calibration to reflectance provides a basis for comparison of reflectance values between adjacent flight lines and between different altitudes. A hybrid model was used to perform this calibration using pseudo-invariant features (PIFs) and an on-board downwelling irradiance sensor (Incident Light Probe (ILP)) (Shepherd, 1994; Shepherd *et al.*, 1995). The CASI data are calibrated to reflectance (32-bit real numbers) but stored as 16-bit integers for more efficient storage and data processing. The relationship between CASI digital number (DN) and reflectance is $Reflectance (R) = (CASI\ DN)^{-6}$.

Digital Elevation Data

The DEM for the study area was produced by the Department of Natural Resources-Forestry Canada. This DEM was generated at a 20-m grid spacing using the ANUDEM procedure (Hutchinson, 1989; Mackey *et al.*, 1994) based on digital topographic data (contours and streamline data) from the 1:20,000-scale Ontario Basic Mapping (OBM) Series.

Methodology

Georeferencing of CASI Data

A georeferenced database for the study area was developed incorporating spectral, spectral-spatial, texture, and terrain variables. A common spatial resolution of 4 m by 4 m was selected for this database, incorporating CASI data as well as the 20-m DEM. CASI reflectance data were registered to a Landsat TM scene that was resampled to 4 m and georeferenced to the Universal Transverse Mercator (UTM) projection at a 4-m pixel spacing. To register the CASI data to a 4-m pixel within the georeferenced dataset, a fourth- or fifth-order polynomial was applied to each flight line to model the distortions inherent in each flight line. Using such high-order polynomials is necessary for correcting distortions caused by aircraft movement and orientation. At the same time, it is understood that using polynomials of such high order can also generate significant distortions in some parts of the image. To minimize this potential, care was taken to select a large number of control points that were well distributed throughout each flight line. The data were then resampled using a nearest-neighbor algorithm. Although the CASI data had been corrected for aircraft roll, registration errors persisted (e.g., mean residuals in the x and y direction of 3 and 7 pixels, respectively). In all, five CASI flight lines were georeferenced and combined with Landsat TM data to form a mosaic covering the entire study area (Figure 1).

CASI Spectral Feature Selection

Band 1 (435 to 466 nm) was eliminated from analysis due to noise and poor dynamic range. Also, it was observed that Bands 8 (785 to 795 nm) and 9 (860 to 888 nm) suffered from poor focus and, therefore, were omitted from this analysis. To reduce the data dimensionality of the remaining six features of

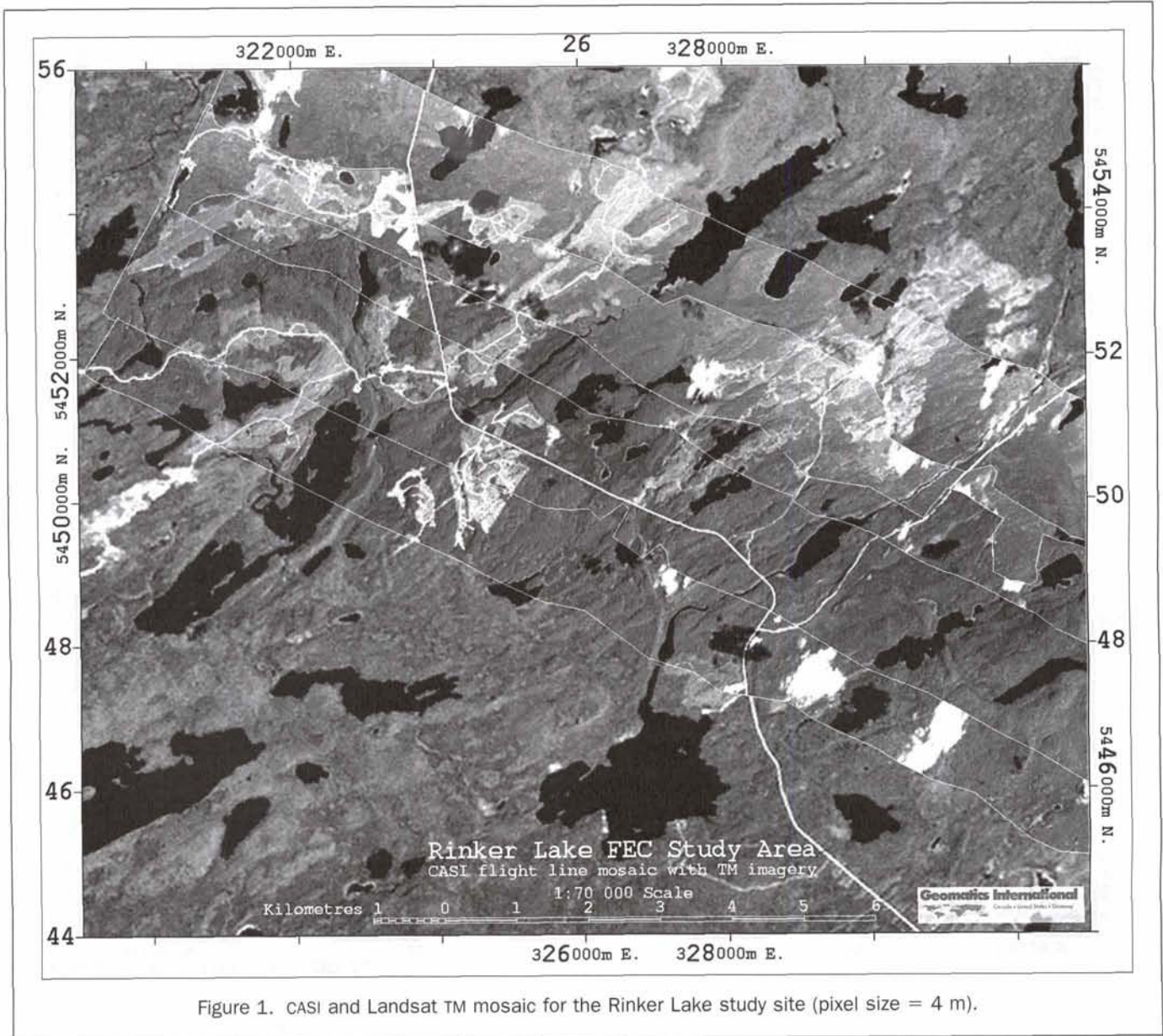


Figure 1. CASI and Landsat TM mosaic for the Rinker Lake study site (pixel size = 4 m).

CASI data, the Jeffries-Matusita (J-M) distance, a statistical separability measure, was used to evaluate candidate feature subsets. J-M distance is a measure of the average difference between the two-class density functions and ranges between 0 and 2 (Swain and Davis, 1978). J-M distance was selected because it, along with transformed divergence, produced superior separability results for image classification over Bhattacharyya distance and simple divergence (Mausel *et al.*, 1990).

Feature selection was applied to the original CASI data because spectral-spatial and texture features would be generated from these original CASI data. In order to keep the number of derived variables to a minimum (i.e., spectral-spatial and texture features), the dimensionality of the original dataset was reduced. Also, because linear discriminant analysis is affected by the number of variables, it was desirable to maintain a minimum number of variables.

CASI features were selected using the following procedure to collect reflectance data for the six landscape-scale ecosystem classes (Treitz *et al.*, 1996):

- (1) FEC plots were located on the georeferenced imagery using GPS coordinates. For each landscape-scale forest ecosystem class,

ten calibration sites (consisting of 25 pixels each) were used to calculate the mean and covariance for each class.

- (2) The number of CASI features was selected from one to six.
- (3) Feature subsets of the specified number of CASI features (i.e., 1, 2, 3, 4, 5, or 6) were determined. For each candidate feature subset, the average J-M distance was calculated for each landscape-scale class pair.
- (4) This process was repeated for each possible combination of the specified number of CASI features identified in Step 2, and the average J-M distance for each feature subset was tracked.
- (5) The maximum of the average J-M distance was used to select the best feature subset for the given number of features desired.
- (6) Steps 2 to 5 were repeated for different numbers of CASI features. These results are reported in Table 4.

J-M distances greater than 1.9 for a two-class density function indicate good separability between those two classes. Values ranging from 1.0 to 1.9 indicate the classes (or subset of classes) are separable to some extent. The J-M distances presented in Table 4 indicate the maximum average pairwise J-M

TABLE 4. FEATURE SELECTION BASED ON JEFFRIES-MATUSITA (J-M) DISTANCE

Number of Features	Features						Maximum J-M Distance Average*
	2	3	4	5	6	7	
1						✓	0.591
2	✓					✓	0.877
3		✓		✓		✓	0.987
4		✓		✓	✓	✓	1.081
5	✓		✓	✓	✓	✓	1.136
6	✓	✓	✓	✓	✓	✓	1.165

distances for the specified number of CASI features and six forest ecosystem classes. Based on this analysis, CASI spectral features (variables) 3, 5, and 7 were selected for spatial averaging to "optimal" spatial resolutions/scales, texture analysis, and integration with terrain variables. Although all six features provided the greatest J-M distance (Table 4), it was decided that the three features providing the highest J-M distance would be selected, in order to maximize J-M distance while maintaining a relatively small number of variables (i.e., for linear discriminant analysis). Each of these features represent important "spectral regions" of the reflectance curve (green peak reflectance, chlorophyll well, and infrared reflectance). It was anticipated that features representative of these regions would also provide the best features for scaling, texture analysis, and integration with terrain features.

Spectral-Spatial Features

Specific spatial resolutions for visible and near-infrared reflectance data were identified for the six landscape-scale ecosystem classes based on semivariogram analysis of sample CASI data collected at 0.70- by 5.36-m spatial resolution (600 m AGL) (Treitz, 1997) (Table 5). Based on the semivariogram analysis of the sample data, a series of spectral-spatial features were derived from the 4-m CASI data (features 3, 5, and 7) using a technique of non-overlapping spatial averaging. With this technique, the mean reflectance within a non-overlapping square window is calculated and assigned to an output image. The input window is then moved a distance equivalent to the window size and a new mean reflectance value is calculated. This process is repeated over the entire image. The 4-m data approximate the lower limits of "optimal" spatial resolutions estimated for specific forest ecosystem classes. For example, the spatial resolution of the CASI

TABLE 5. "OPTIMAL" SPATIAL RESOLUTION CASI DATASET BASED ON SEMIVARIOGRAM ANALYSIS (FROM TREITZ (1997))

CASI Spectral Variable	Spatial Resolution	Landscape Level Ecosystem Classes*					
		1	2	3	4	5	6
CASI (580-601 nm)	4 meters					✓	✓
	5 meters						
	6 meters	✓	✓	✓	✓		
CASI (663-678 nm)	4 meters					✓	✓
	5 meters				✓	✓	
	6 meters	✓	✓				
CASI (744-750 nm)	5 meters					✓	✓
	6 meters			✓	✓		
	7 meters	✓	✓				

*1. Aspen-Dominated Hardwood and Mixedwood; 2. White Spruce/Balsam Fir Conifer and Mixedwood; 3. Cedar Mixedwood; 4. Upland Black Spruce/Jack Pine; 5. Lowland Black Spruce; and 6. Wetland Black Spruce

data used in this analysis (i.e., 3.18 m by 5.36 m or 17 m² and subsequently resampled to 4 m by 4 m or 16 m² during georeferencing) approximates the "optimal" spatial resolution estimated from CASI data collected at 600 m AGL (i.e., 0.7 m by 5.36 m or 16 m²) for Lowland/Wetland Black Spruce using semivariogram analysis. "Optimal" spatial resolutions often differed between landscape-scale ecosystem classes and between visible and near infrared wavelengths.

To simulate datasets at 5, 6, and 7 meters spatial resolution, a one-meter database was developed from the original CASI data, meaning that the original database of 4-m spatial resolution (3500 pixels by 3000 lines) was written to a database of 14,000 pixels by 12,000 lines. CASI Bands 3 and 5 were then spatially averaged to 5 m and 6 m while CASI Band 7 was averaged to 5-, 6-, and 7-m spatial resolutions. These spatial resolutions reflect the results of the semivariogram analysis, with the optimal resolutions being larger for the near-infrared data than for the visible (Treitz, 1997).

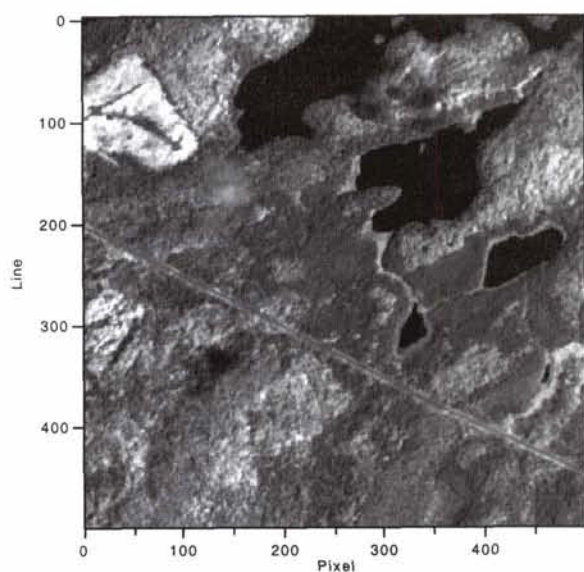
Although it is unclear how closely spatial averaging simulates multi-spatial resolution remote sensing data, it has been demonstrated to be superior to algorithms such as cubic convolution and bilinear interpolation for upscaling spectral signals (Hay *et al.*, 1997). Non-overlapping spatial averaging assumes that smaller-scale systems behave similarly to the average of larger-scale systems. However, differing structural patterns occur within the landscape at various scales and do not necessarily interact in a linear fashion. The 5-, 6-, and 7-m CASI datasets were then georeferenced to the 4-m dataset using a first-order polynomial and nearest-neighbor resampling algorithm. Sub-areas representing spatially averaged features for Band 7 (744 to 750 nm) are presented in Figure 2.

Texture Features

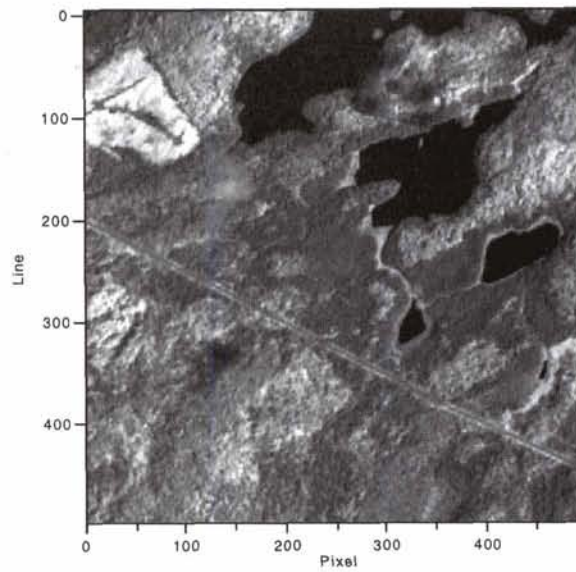
Here, texture analysis is examined as an important contributor to scene information extraction. Texture may contain important information about the structural arrangement of surfaces and their relationships to the surrounding environment (Haralick *et al.*, 1973). It has been shown that classification accuracies are improved when texture features are incorporated into image classification (Peddle and Franklin, 1991; Barber *et al.*, 1993; Rotunno *et al.*, 1996). In this study, the gray-level co-occurrence matrix (GLCM) statistical method is used to generate texture features from the CASI data.

The GLCM method can be defined as a matrix of relative frequencies in which two neighboring pixels, separated by distance δ and having an angular relationship α , occur on the image, one with gray tone i , and the other with gray tone j (Haralick *et al.*, 1973). The power of the GLCM approach is that it characterizes the spatial interrelationships of the gray tones in a textural pattern and can do so in a way that is invariant under monotonic gray-tone transformations. On the other hand, it does not capture the shape aspects of the tonal primitives and, therefore, is not well-suited for textures composed of large-area primitives (Haralick 1979). Hence, this technique is suited to the CASI data analyzed in this study (i.e., L-resolution data as defined by Strahler *et al.*, 1986). The objective of these statistical approaches is to translate visual properties into quantitative descriptors in a manner that they can be used to discriminate relevant land features using additional image processing techniques.

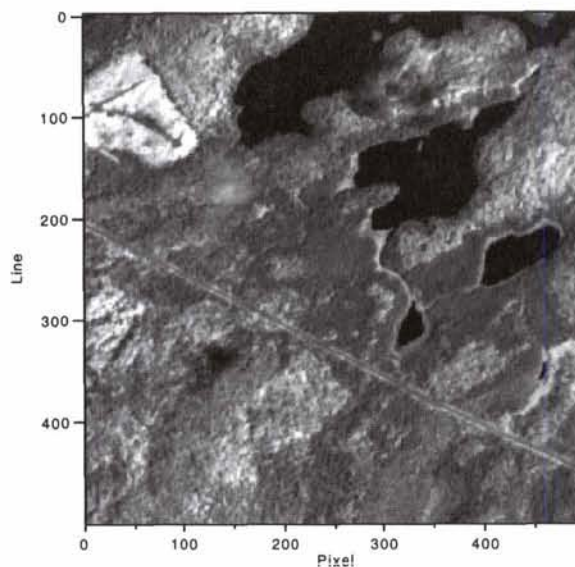
GLCM analysis was performed on a 6-bit linear transformation of the original 16-bit CASI data using measures of contrast, mean, and correlation. Quantization-level scaling is performed to increase computational efficiency during matrix calculations. These analyses were performed on CASI visible (580 to 601 nm) and near-infrared (744 to 750 nm) data. Texture features (mean, contrast, and correlation) (Figure 3) based on GLCMs were generated using EASI/PACE software (PCI, 1997): i.e.,



0 5000 10000 15000 20000 25000
CASI Reflectance (744 - 750 nm) Spatial Resolution = 5 m



0 5000 10000 15000 20000 25000
CASI Reflectance (744 - 750 nm) Spatial Resolution = 6 m



0 5000 10000 15000 20000 25000
CASI Reflectance (744 - 750 nm) Spatial Resolution = 7 m

Figure 2. Spectral-spatial features for CASI Band 7 reflectance at different spatial resolutions (744 to 750 nm).

Mean

$$\sum_{i=1}^n \sum_{j=1}^n (C_{ij}) \cdot i$$

Contrast

$$\sum_{i=1}^n \sum_{j=1}^n C_{ij}(i - j)^2$$

Correlation

$$\sum_{i=1}^n \sum_{j=1}^n C_{ij} \frac{(i - \mu_i)(j - \mu_j)}{\sigma_i \sigma_j}$$

where

C_{ij} is the ij th entry of the co-occurrence matrix,
 n is the number of pixel pairs in the image at (δ, α) ,
 i is the gray-level intensity value of the i th reference row,
 j is the gray-level intensity value of the j th neighbor column,

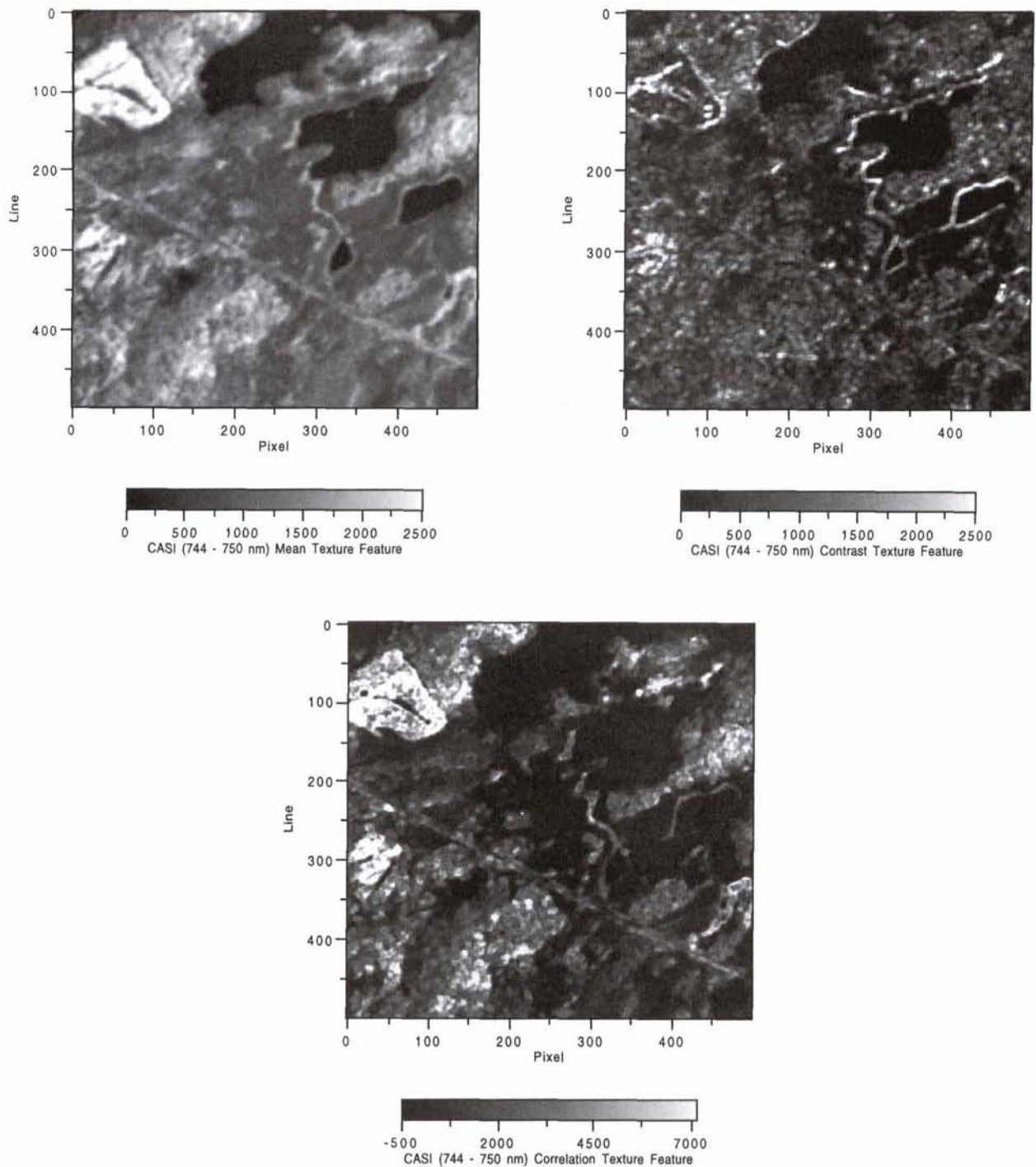


Figure 3. Mean, contrast, and correlation texture features for CASI Band 7 (744 to 750 nm).

μ_i is the mean of row i ,
 μ_j is the mean of column j ,
 σ_i is the standard deviation of row i , and
 σ_j is the standard deviation of column j .

Although these features measure the same characteristics of the data (i.e., texture), they are interpreted differently. The mean texture statistic incorporates both tone and texture information. This is achieved by incorporating the gray level of the i th line of the matrix in the texture calculation. The contrast statistic is a measure of the amount of local variation present in an

image (Haralick *et al.*, 1973; Ulaby *et al.*, 1986; Pultz and Brown, 1987). Contrast is a measure that is associated with the average gray-level difference between neighboring pixels and is sensitive to standard deviation but not mean (Barber, 1989). A low-contrast image results in a concentration of entries around the diagonal of the GLCM and, consequently, a low value for the computed contrast statistic (Baraldi and Parmiggiani, 1995). The correlation statistic is analogous to Pearson's product moment correlation and is sensitive to the correlation between gray values and the probability density functions at each of the

gray-level pairs. The correlation texture statistic is sensitive to both mean and standard deviation (Barber, 1989).

In generating each of these texture features, three parameters must be selected. These include (1) window size for which the co-occurrence matrix will be generated, (2) interpixel sampling distance, and (3) direction for pixel co-occurrence within the sampling window. For feature generation, an appropriate window size is one that is large enough so that a meaningful joint distribution of gray tones can be computed to characterize specific land covers, yet is small enough to minimize the transitional effects of the texture calculation at boundaries between adjacent classes. Because the "optimal" spatial resolutions determined for the visible and near-infrared data were different (Treitz, 1997), a 5- by 5-pixel window was used for generating the GLCM for the visible data (580 to 601 nm) and a 7- by 7-pixel window for the near-infrared data (744 to 750 nm). These window sizes were selected for application to the 2630-m AGL CASI data to account for the differences between the visible and near-infrared data and to generate a meaningful joint distribution of gray tones. However, it must be noted that optimal textural window operators were based on semivariogram analysis of CASI data collected at 600 m AGL, thereby possessing a spatial resolution of 0.73 m by 5.36 m (Treitz, 1997). These estimates portray smaller spatial dimensions than are used here for the 2630-m AGL CASI data. It is accepted that the relationship between reflectances of the 600-m and 2630-m AGL CASI data is not likely to be linear. In this respect, based on semivariogram analysis of the 600-m AGL CASI data, the texture processing of the 2630-m AGL data addresses texture at a smaller scale than was observed in the 600-m AGL CASI data.

The inter-pixel sampling distance (δ) is selected based on the coarseness or fineness of the textures present in the image. For example, for fine-texture features, a short inter-pixel sampling distance would be suitable, whereas a greater distance would be appropriate for coarse-textured images. However, because there are generally a variety of degrees of fineness and coarseness within an image, an inter-pixel sampling distance of one ($\delta = 1$) is valid to characterize different degrees of texture.

Haralick *et al.* (1973) proposed calculating second-order statistics for the co-occurrence matrix in four directions ($\alpha = 0^\circ, 45^\circ, 90^\circ, 135^\circ$). If the objective is to create invariant features after rotation, this method is appropriate (Vickers and Modestino, 1982). However, in a study by Franklin and Peddle (1989), it was observed that individual texture orientations produced higher class accuracies than did average texture measures using the four orientations. In this study, one directional measure was used (i.e., $\alpha = 0$). Here, the evaluation of the GLCM technique is based on the discrimination of the six landscape-scale forest ecosystem classes from these texture features. Texture features generated from the GLCM are classified individually and in combination using a linear discriminant function.

Geomorphometric Processing

Two first-order derivatives of altitude (gradient and local relief) were derived from the elevation model. A gradient image portrays the rate of maximum change in elevation between neighboring cells (0 to 90°). Degree gradient for any given cell in the matrix is calculated as the gradient of a plane formed by the vectors connecting the neighboring cells in a 3- by 3-cell window, where each cell contains an elevation value. The gradient image was derived using the algorithms implemented in ARC/INFO (ESRI, 1996). To quantify the local variability in elevation and gradient, a map of local relief was generated by calculating the range of altitude within a 5- by 5-pixel moving window. This feature effectively portrays the maximum change in altitude within a 100- by 100-m (1-ha) area and represents a first-order statistical derivative of elevation. A sub-area depicting the three terrain features—elevation, gradient, and local relief—is presented in Figure 4.

Forest Ecosystem Reflectance Data Collection

For this study, detailed V-Types were aggregated to six landscape-scale ecosystem classes that were present in the Rinker Lake Study Area (Table 1). Here, detailed V-Types were aggregated to coarser ecological units based on (1) "Treatment Units" (Racey *et al.*, 1989) which are groupings determined by similar soil moisture and nutrient regimes and (2) observed vegetation associations in the field. Forest ecosystem plot data were then aggregated into the six landscape-scale forest ecosystem classes. Based on this grouping, sites were located in the CASI image data. Only sites that could be accurately located, and fell within a relatively large homogeneous area, were selected for analysis. A sample consisting of 1500 calibration pixels and 1500 validation pixels (250 calibration and validation pixels per sample for each of the six classes) was collected.

Forest ecosystem plots were located on the georeferenced imagery using GPS coordinates. Due to the error observed in the registration process, these positions were checked against 1:8,000-scale color-infrared photographs and distance and direction measurements used in the field. For each landscape-scale forest ecosystem class, 20 sites were located for a total of 120 sites. For each site, a 20- by 20-m area, corresponding to 25 pixels, was extracted from the CASI image dataset and used in the calculation of mean and covariance for each class.

In cases where there were only a few forest stands of a particular landscape-scale forest ecosystem class (i.e., cedar mixedwood and wetland black spruce), attempts were made to collect calibration and validation data from separate stands or from the same stand on different flight lines. When this was not possible, samples were taken from different locations within the stand.

Linear Discriminant Analysis (LDA)

Linear discriminant analysis (LDA) procedures were applied within SYSTAT™ (SYSTAT Inc., 1992) to explore the relative discriminatory power of the (1) spectral-spatial, (2) texture, (3) terrain, and (4) combinations of spectral-spatial, texture, and terrain variables. According to Duda and Hart (1973), LDA does not have a rigorous requirement for an underlying statistical model. In this sense, LDA is not seriously affected by limited deviations from normality or limited inequality of variances (Davis, 1986). In this analysis, Fisher's method, which is based on a single within-groups covariance matrix derived from calibration data, is applied (SYSTAT Inc., 1992). This method first derives a transform that minimizes the ratio of the difference between group multivariate means and their within-group multivariate variance. This transform is used to find a discriminant function as the orientation that optimizes the separability of classes while at the same time minimizing the internal spread of each individual class distribution (Tom and Miller, 1984). An input pixel is then assigned to a particular class based on its location along the discriminant function axis. Discriminant analysis as a classification technique has been shown to be less sensitive to the number of variables and deviations from the normal (Gaussian) distribution as opposed to other methods such as maximum likelihood (Tom and Miller, 1984).

The variable sets used in this analysis are defined in Table 6. The minimum number of variables for any trial was one, the maximum, nine. For each set of variables, calibration data were used to generate a discriminant function, which was then applied to the validation data to obtain individual and mean class accuracies. The Kappa coefficient (κ) was calculated for the validation accuracies of each classification. The Kappa coefficient is a measure of agreement between the ground sample classes and those derived through classification of spectral, spatial, texture, and/or terrain features. This measure accounts for all elements of the confusion matrix and excludes the agreements that occur by chance (Rosenfield and Fitzpatrick-Lins, 1986). Difference-of-proportions tests (Freund and Simon,

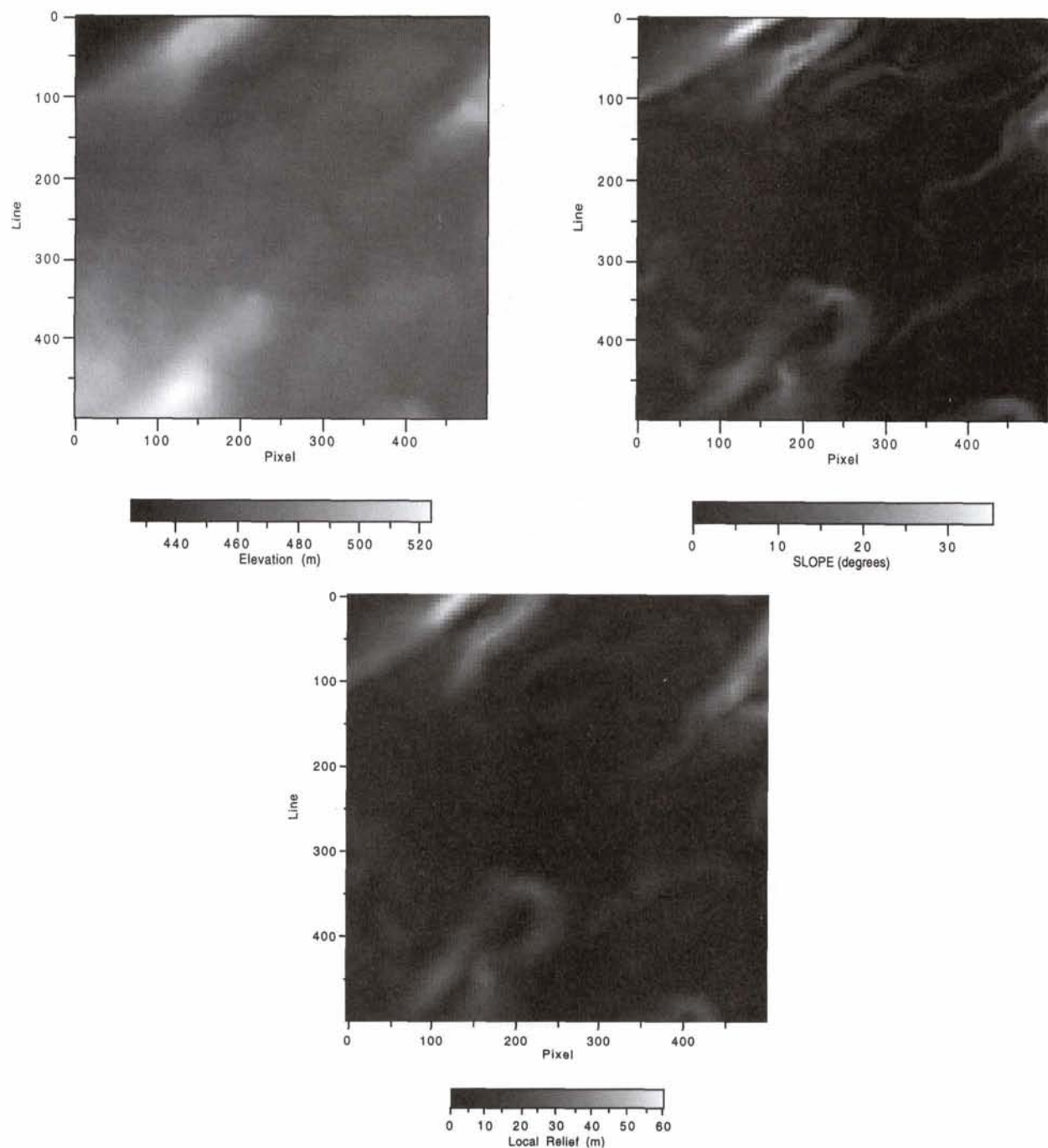


Figure 4. Elevation, gradient, and local relief terrain variables for a sub-area of the Rinker Lake study site (pixel size = 4 m).

1992) were performed to determine the significance of the differences between classification accuracies for the various combinations of input variables.

Results

The CASI 6-m dataset (SPAC) provided the highest accuracies among the spectral-spatial variables and were significantly greater than the 4-m data set (SPEB) ($z = 3.88$). The 6-m data (SPAC) also provided greater discrimination of the six landscape-scale classes than did the "optimal" spatial resolution

dataset (SPAA), the 5-m dataset (SPAB), and the 6-m and 7-m dataset (SPAD) (Table 7).

Among the texture datasets, TEXTF provides the highest classification accuracy, significantly greater than TEXA ($z = 3.47$) and TEXC ($z = 2.84$), as well as all spectral-spatial and terrain feature datasets (Table 7). The texture dataset, TEXTF, which incorporates six texture features, does not provide significant improvement in classification accuracy over TEXTB, a three-texture feature dataset ($z = 0.87$). Of the three-texture features tested, the mean-texture feature provides the greatest discrimination, followed by contrast and correlation.

TABLE 6. FEATURE DATASETS FOR LINEAR DISCRIMINANT ANALYSIS

Variable Set	Description
<i>Spectral</i>	
SPEA	CASI Bands 3, 5, 7
<i>Spectral-Spatial</i>	
SPAA	Optimal Spatial Resolutions by class (4m, 5m, 6m and 7m) for CASI Bands 3, 5 and 7
SPAB	CASI Bands 3, 5, and 7 at 5 meter spatial resolution
SPAC	CASI Bands 3, 5, and 7 at 6 meter spatial resolution
SPAD	CASI Bands 3, 5 (6m) and Band 7 (7m)
<i>Texture</i>	
TEXA	Texture Statistics: Mean—Bands 3 and 7
TEXB	Texture Statistics: Mean—Bands 3 and 7; Contrast—Band 7
TEXC	Texture Statistics: Mean—Bands 3 and 7; Correlation—Band 7
TEXD	Texture Statistics: Mean—Bands 3 and 7; Contrast and Correlation—Band 7
TEXE	Texture Statistics: Mean, Contrast—Bands 3 and 7; Correlation—Band 7
TEXF	Texture Statistics: Mean, Contrast, Correlation—Bands 3 and 7
<i>Terrain</i>	
DEM	Digital Elevation Model (DEM)
REL	Local Relief Elevation (range within 100m x 100m window)
GRAD	Gradient
TERA	Local Relief and DEM
TERB	Local Relief, DEM and Gradient
<i>Integrated</i>	
INTA	SPAC and TEXB
INTB	SPAC and TERB
INTC	SPAC, TERB and TEXB

Terrain variables by themselves do not provide significant discrimination of any of the six landscape-scale classes. However, of the four terrain variables tested, elevation (DEM) provides the best discrimination, significantly greater discrimination than other single terrain variables. In combination, elevation, gradient and local relief (TERB) provide a slight improvement over DEM alone; however, it is not significant ($z = 0.07$).

Finally, integrating spectral-spatial, texture, and terrain variables (INTC) provides the greatest discrimination of the six landscape-scale ecosystem classes, significantly greater than all other datasets (Table 7). When spectral-spatial variables are combined with either texture variables (INTA) or terrain variables (INTB) alone, the results are not significantly different from using texture features alone (e.g., TEXB) ($z = 0.60$ and 0.41 , respectively).

When examining the individual class accuracies, it is evident that upland black spruce/jack pine is consistently poorly classified. Of the variables tested, there is no variable that provides the discrimination of upland black spruce/jack pine. Similarly, the white spruce/balsam fir landscape-scale class is poorly discriminated. The accuracies for the remaining four landscape-scale classes range from 77.2 percent to 93.2 percent (Table 7).

Discussion

Aspen-dominated hardwood and mixedwood, cedar mixedwood, lowland black spruce, and wetland black spruce are the classes most easily discriminated whereas upland black spruce/jack pine and white spruce/balsam fir are more difficult. If the discrimination of the latter two landscape-scale classes could be improved, the overall results would improve significantly. It is not by chance that these two classes represent the most variable of conditions, both spectrally, spatially, and in reference to the terrain. Here, it should be noted that classification accuracy is a function not only of technique, but also of the class structure used with respect to the spatial and radio-

TABLE 7. CLASSIFICATION ACCURACY (LINEAR DISCRIMINANT FUNCTION) BY CLASS

Variable Set†	Percent Classification Accuracy by Class**						Mean Accuracy (%)	Kappa Coefficient (\hat{K})
	1	2	3	4	5	6		
<i>Spectral</i>								
SPEA	78.4	33.2	41.2	14.0	63.2	71.6	50.3	0.403
<i>Spectral-Spatial</i>								
SPAA	72.4	32.4	62.8	15.2	63.6	68.4	52.5	0.430
SPAB	78.0	38.4	58.4	14.0	66.4	80.0	55.9	0.470
SPAC	72.4	36.8	63.6	17.2	75.6	78.4	57.3	0.488
SPAD	72.0	36.8	57.2	15.6	76.4	76.4	55.7	0.469
<i>Texture</i>								
TEXA	70.8	25.6	54.0	29.6	73.6	89.2	57.1	0.486
TEXB	70.8	31.6	56.0	36.4	86.8	89.2	61.8	0.542
TEXC	78.4	19.2	66.0	25.2	80.4	80.4	58.3	0.499
TEXD	81.2	18.4	67.6	30.4	88.0	80.0	60.9	0.531
TEXE	80.8	18.0	64.8	31.6	86.8	93.2	62.5	0.550
TEXF	78.0	18.4	64.8	40.0	84.4	94.4	63.3	0.560
<i>Terrain</i>								
DEM	10.0	40.0	70.0	20.0	60.0	67.2	44.5	0.334
REL	24.0	21.6	54.0	15.6	32.4	76.4	37.3	0.248
GRAD	30.0	10.0	56.0	2.0	26.8	89.2	35.7	0.228
TERA	20.0	40.0	70.0	0.0	60.0	70.0	43.3	0.320
TERB	28.0	40.0	70.0	0.0	60.0	70.0	44.7	0.336
<i>Integrated</i>								
INTA	70.4	44.8	76.4	21.6	85.2	78.8	62.9	0.554
INTB	77.6	43.2	78.8	14.0	81.6	80.0	62.5	0.550
INTC	77.2	46.4	85.2	23.6	93.2	80.0	67.6	0.611

*Values in bold represent the highest classification accuracies for each class.

†Acronyms are defined in Table 6.

**1. Aspen-Dominated Hardwood and Mixedwood; 2. White Spruce / Balsam Fir Conifer and Mixedwood; 3. Cedar Mixedwood; 4. Upland Black Spruce / Jack Pine; 5. Lowland Black Spruce; and 6. Wetland Black Spruce

metric precision of the data (Hutchinson, 1982). These two classes in particular require close examination as to the conditions under which they may be uniquely characterized, either spectrally, spatially, or with reference to more specific terrain characteristics. It is likely that examination of these two classes from a class perspective is required, in that they may require further segregation or aggregation in order to consider them as mappable units or classes. The remaining four classes appear to be discriminable at appropriate levels, although these may also require reorganization to improve discriminability while maintaining ecological significance.

In terms of the spectral-spatial variables used to map the six landscape-scale classes, the dataset consisting of three CASI spectral bands at a spatial resolution of 6-m (SPAC) provided the best discrimination when compared to other spectral-spatial variables. The differences were not great, but were statistically significant. The dataset combining 6-m and 7-m data had a slightly lower LDA classification accuracy than did the 6-m dataset, suggesting that the optimal resolution was exceeded. On the other hand, the dataset that combined 4-, 5-, 6-, and 7-m data, did not produce the best results among the spectral-spatial variables. This may be linked to the fact that the estimates derived from the semivariogram analysis represent the mean sizes of support for a number of transects taken from each of the six landscape-scale classes. Possibly it would be more prudent to over-estimate the size of support based on the experimental variograms in order to optimally regularize the variability within the six landscape-scale classes. There may be some relationship between the mean size of support and maximum size of support observed from a sample of experimental variograms to optimally determine the spatial resolution per class. This estimate then may best account for the spatial variability within the class. The estimate may not necessarily have the same relationship to the mean for each class, but may vary based on the level of variability of each class. Regardless, it seems apparent that selecting an optimal spatial resolution for spectral data collection alone does not provide sufficient discriminatory power for classifying and mapping the six landscape-scale classes studied here. With the spatial resolutions examined, there is still significant within-class variability to contribute to poor between-class separability.

Texture variables provide accuracies equal to, or greater than, any of the spectral-spatial variables. This supports the assertion that texture information is present within these L-resolution reflectance data and is characterized to some degree by second-order texture transforms to assist in the discrimination of these landscape-scale classes. In addition, the mean texture feature provided the greatest discrimination among the classes because it not only characterizes texture, but it contains tonal (spectral) information as well. Mean texture features combined with the contrast texture feature for CASI Band 7 (744 nm to 750 nm) contributes additional textural information to provide additional discrimination for the forest ecosystem classes using three texture variables. It is suggested that these texture variables not only capture the tonal differences between general ecosystem classes, but that, within general ecosystem classes, they capture forest stand density differences. For example, texture variables improve the discrimination between lowland black spruce and lowland/wetland black spruce. This may be attributed to the contrasting stem densities of 1700 stems/ha and 900 stems/ha for lowland black spruce and lowland/wetland black spruce, respectively. Aspen-dominated stands, which possess the lowest stand densities (<700 stems/ha), are also well discriminated using textural features. This would suggest that texture variables may be extremely useful in characterizing forest stand structure (e.g., stem density, canopy closure) at spatial resolutions where individual objects are not resolvable.

It is evident that the terrain features tested here (i.e., eleva-

tion, local relief, and gradient) do not provide great discriminatory power for the six landscape-scale classes examined. However, it does appear that, within a small region, local elevation and gradient can be used to assist in the discrimination of forest ecosystem classes when combined with other descriptors. It must be emphasized that, for a low- to moderate-relief boreal environment, these variables, particularly elevation, would have to be used within a relatively small local area, emphasizing the local variation between ecosystem types. Gradient, on the other hand, may have potential for use at more regional scales.

Based on the analyses presented, the integration of spectral data collected at appropriate resolutions with terrain information and texturally processed features offers promise for discriminating and classifying forest ecosystem classes. When the three types of variables were combined (INTC), a mean classification accuracy of 67.6 percent ($\kappa = 0.611$) was achieved using LDA. Although this does not approach operational levels, it indicates that spectral, spatial, and terrain variables, in combination, offer potential for discriminating forest ecosystems classes in low- to moderate-relief boreal environments. However, it appears that, in this boreal environment, application of geomorphometric variables derived from 1:20,000-scale map data with a 5-m contour interval does not provide sufficient discrimination for the forest ecosystems examined. Based on field observations, elevation differences as small as a meter in this bedrock controlled environment could produce contrasting moisture regimes and, hence, vegetation patterns at close proximity to each other. Given that the root-mean-square error of DEMs derived from contours is approximately one-third to one-fifth of the contour interval, the difficulty in associating terrain variables with vegetation associations in a low- to moderate-relief boreal environment such as this is problematic. The reader is referred to numerous articles detailing the accuracy of digital elevation/terrain models (e.g., Chang and Tsai, 1991; Robinson, 1994; Giles and Franklin, 1996; Florinsky, 1998).

Further refinements in spectral-spatial, textural, and terrain variables may provide the necessary discrimination required for operational classification and mapping of large areas of northern boreal forest. Specifically, improvement in discriminating certain ecosystem types such as upland black spruce/jack pine and white spruce/balsam fir conifer and mixedwood would increase significantly the potential for classification and mapping. It is suggested that more detailed terrain data modeling soil nutrient and moisture regimes are necessary for incorporation with reflectance and textural data for discriminating forest ecosystems. Additional potential lies with estimating structural variables from spectral-spatial and textural features.

Conclusions

Given the relationship between forest and site, it was hypothesized that combining appropriately scaled remote sensing data with terrain descriptors/variables should improve the discriminability of landscape-scale forest ecosystem classes for the boreal forest of northwestern Ontario, Canada. Although not completely encouraging in terms of absolute classification accuracies, various conclusions can be made regarding (1) optimal scales of remote sensing data, (2) texture processing, and (3) the integration of terrain variables with reflectance data for discriminating forest ecosystem classes in a low- to moderate-relief boreal environment. These include

- Careful consideration must be given to the relationships between the forest classes of interest and the appropriate remote sensing spatial resolutions at which to sample those classes. To maximize discriminability of forest ecosystem classes, a spatial resolution that minimizes (regularizes) within-class variability, but maximizes between-class discrimination is required. Here it was demonstrated that 6-m reflectance data

provided the best discrimination of the landscape-scale forest ecosystem classes studied. This spatial resolution or scale provided greater discrimination than the following spectral-spatial datasets: (1) a 5-m dataset; (2) a combined dataset of 6- and 7-m data; and (3) an "optimal" dataset (by class) of 4-, 5-, 6-, and 7-m data. However, multiple spatial resolutions/scales of remote sensing reflectance data may be required, depending on the nature of the classes to be discriminated and their structure, as well as their characteristic visible and near-infrared reflectance.

- *Texture features derived from L-resolution CASI reflectance data provide significant information for discrimination of landscape-scale forest ecosystem classes.* Here, texture variables provide accuracies equal to, or greater than, any of the spectral-spatial variables. It is clear that texture information is present within these L-resolution reflectance data and is characterized to some degree by GLCM texture transforms to assist in the discrimination of these landscape-scale forest ecosystem classes.
- *Terrain variables alone provide weak discrimination of forest ecosystem classes. However, when used in combination with spectral-spatial variables, they improve the discrimination of landscape-scale forest ecosystem classes.* It must be emphasized that for a low- to moderate-relief boreal environment, these variables, particularly elevation, would have to be used within a relatively small local area, emphasizing the local variation between ecosystem types. Slope, on the other hand, may have potential for use at more regional scales. It is postulated that more precise descriptors or models of terrain are required for integration with appropriate spectral-spatial reflectance features in a low- to moderate-relief boreal environment. These features must be derived from geomorphometric and soils data to model soil texture classes and moisture and nutrient regimes.
- *The integration of spectral data collected at appropriate resolutions with terrain information and texturally processed features offers promise for discriminating and classifying forest ecosystem classes.* A mean classification accuracy of 67.6 percent ($\kappa = 0.611$) was achieved when combining spectral-spatial, textural, and terrain variables. This represents a significant improvement over using spectral-spatial, texture, or terrain variables alone or in combinations of two variable types. This level of accuracy is not sufficient for operational classification and mapping, but it does indicate that appropriately scaled spectral, textural, and terrain variables provide a basis for classification and mapping of large forest regions based on ecological criteria.

It has been demonstrated that in a low-relief boreal environment, addition of textural and geomorphometric variables to high-resolution airborne remote sensing reflectance data provides improved discrimination of forest ecosystem classes. Although these improvements are statistically significant, the absolute classification accuracies are not yet at levels suitable for operational classification and mapping. Further refinements, particularly of forest ecosystem class structure and terrain descriptors, are required for operational mapping of forest ecosystem classes.

Acknowledgments

Funding for this research has been provided through the Northern Ontario Development Agreement, Northern Forestry Program. Several agencies contributed to the success of the field program, including Canadian Forest Service—Natural Resources Canada; Northwest Region Science and Technology Unit—Ontario Ministry of Natural Resources; Earth-Observations Laboratory—Centre for Research in Earth and Space Technologies (CRESTech); and the Provincial Remote Sensing Office—Ontario Ministry of Natural Resources. Additional financial support was provided through the University of Waterloo (scholarships and teaching assistantships), the Natural Sciences and Engineering Research Council of Canada (NSERC)—Research Grants awarded to Philip Howarth and Paul Treitz, and the Undergraduate Student Research Awards program, and the Environmental Youth Corps program funded by the Ontario Ministry of Natural Resources.

References

- Babey, S., and R. Soffer, 1992. Radiometric calibration of the compact Airborne Spectrographic Imager (CASI), *Canadian Journal of Remote Sensing*, 18(4):233–242.
- Baraldi, A., and F. Parmiggiani, 1995. An investigation of the textural characteristics associated with gray level co-occurrence matrix statistical parameters, *IEEE Transactions on Geoscience and Remote Sensing*, 33(2):293–304.
- Barber, D., 1989. *Texture Measures for SAR Sea Ice Discrimination: An Evaluation of Univariate Statistical Distributions*, Earth-Observations Laboratory, Institute for Space and Terrestrial Science Technical Report, ISTS-EOL-TR89-005, Department of Geography, University of Waterloo, Ontario, Canada, 56 p.
- Barber, D.G., M.E. Shokr, R.A. Fernandes, E.D. Soulis, D.G. Flett, and E.F. LeDrew, 1993. Comparison of second-order classifiers for SAR sea ice discrimination, *Photogrammetric Engineering & Remote Sensing*, 59(9):1397–1408.
- Cain, D.H., K. Ritters, and K. Orvis, 1997. A multi-scale analysis of landscape statistics, *Landscape Ecology*, 12:199–212.
- Chang, K.-t., and B.-w. Tsai, 1991. The effect of DEM resolution on slope and aspect mapping, *Cartography and Geographic Information Systems*, 18(1):69–77.
- Cohen, W.B., and T.A. Spies, 1992. Estimating structural attributes of Douglas-Fir/Western Hemlock forest stands from Landsat and SPOT imagery, *Remote Sensing of Environment*, 41:1–17.
- Damman, A.W.H., 1979. The role of vegetation analysis in land classification, *Forestry Chronicle*, 55(5):175–182.
- Davis, J.C., 1986. *Statistics and Data Analysis in Geology, Second Edition*, John Wiley and Sons, New York, N.Y., 646 p.
- Duda, R.O., and P.E. Hart, 1973. *Pattern Classification and Scene Analysis*, John Wiley and Sons, New York, 482 p.
- Ekstrand, S., 1996. Landsat TM-based forest damage assessment: Correction for topographic effects, *Photogrammetric Engineering & Remote Sensing*, 62(2):151–161.
- ESRI Inc., 1996. *ArclInfo Users Manual, Version 7*, Environmental Systems Research Institute Inc., 380 New York Street, Redlands, California, variously paged.
- Florinsky, I.V., 1998. Combined analysis of digital terrain models and remotely sensed data in landscape investigations, *Progress in Physical Geography*, 22(1):33–60.
- Florinsky, I.V., and G.A. Kuryakova, 1996. Influence of topography on some vegetation cover properties, *Catena*, 27:123–141.
- Frank, T.D., 1988. Mapping dominant vegetation communities in the Colorado Rocky Mountain Front Range with Landsat Thematic Mapper and digital terrain data, *Photogrammetric Engineering & Remote Sensing*, 54:1727–1734.
- Franklin, S.E., and D.R. Peddle, 1989. Spectral texture for improved class discrimination in complex terrain, *International Journal of Remote Sensing*, 10(8):1437–1443.
- Franklin, S.E., and G.J. McDermid, 1993. Empirical relations between digital SPOT HRV and CASI spectral response and lodgepole pine (*Pinus contorta*) forest stand parameters, *International Journal of Remote Sensing*, 14(12):2331–2348.
- Franklin, S.E., D.R. Connery, and J.A. Williams, 1994. Classification of alpine vegetation using Landsat Thematic Mapper, SPOT HRV and DEM data, *Canadian Journal of Remote Sensing*, 20(1):49–56.
- Freund, J.E., and G.A. Simon, 1992. *Modern Elementary Statistics, Eighth Edition*, Prentice-Hall, Englewood Cliffs, New Jersey, 578 p.
- Giles, P.J., and S.E. Franklin, 1996. Comparison of derivative topographic surfaces of a DEM generated from stereoscopic SPOT images with field measurements, *Photogrammetric Engineering & Remote Sensing*, 62(10):1165–1171.
- Gong, P., R. Pu, and J. Chen, 1996. Mapping ecological land systems and classification uncertainty from digital elevation and forest-cover data using neural networks, *Photogrammetric Engineering & Remote Sensing*, 62:1249–1260.
- Gower, J.F.R., G.A. Borstad, C.D. Anger, and H.R. Edell, 1992. CCD-based imaging spectrometry for remote sensing: The FLI and CASI programs, *Canadian Journal of Remote Sensing*, 18(4):199–208.

- Haralick, R.M., 1979. Statistical and structural approaches to texture, *Proceedings of the IEEE*, 67(5):786-804.
- Haralick, R.M., K. Shanmugam, and I. Dinstein, 1973. Texture features for image classification, *IEEE Transactions on Systems, Man, and Cybernetics*, 3(6):610-621.
- Hay, G.J., K.O. Niemann, and D.G. Goodenough, 1997. Spatial thresholds, image-objects, and upscaling: A multiscale evaluation, *Remote Sensing of Environment*, 62:1-19.
- Hills, G.A., and G. Pierpoint, 1960. *Forest Site Evaluation in Ontario*, Research Report, No. 42, Ontario Department of Lands and Forests, Toronto, Ontario, 63 p.
- Hutchinson, C., 1982. Techniques for combining Landsat and ancillary data for digital classification improvement, *Photogrammetric Engineering & Remote Sensing*, 48(1):123-130.
- Hutchinson, M.F., 1989. A new procedure for gridding elevation and stream line data with automatic removal of pits, *Journal of Hydrology*, 106:211-232.
- Kalnins, V.J., P.M. Treitz, and P.J. Howarth, 1994. *Rinker Lake Data Report 1993-1994*, Technical Report ISTS-EOL-TR94-002, Earth-Observations Laboratory, Waterloo, Ontario, variously paged.
- Mackey, B.G., R.A. Sims, K.A. Baldwin, and I.D. Moore, 1996. Spatial analysis of boreal forest ecosystems: Results from the Rinker Lake case study, *GIS and Environmental Modeling: Progress and Research Issues* (M.F. Goodchild, L.T. Steyaert, B.O. Parks, C. Johnston, D. Maidment, M. Crane, and S. Glendinning, editors), GIS World Inc., Fort Collins, Colorado, pp. 187-190.
- Mausel, P.W., W.J. Kamber, and J.K. Lee, 1990. Optimal band selection for supervised classification of multispectral data, *Photogrammetric Engineering & Remote Sensing*, 56(1):55-60.
- McLean, N.H., and P.W. Uhlig, 1987. *Field Methods Training Manual for the Northwest Region FEC*, Ontario Ministry of Natural Resources (OMNR), Toronto, Canada, unpublished report, 28 p. plus three appendices.
- Michaelsen, J., D.S. Schimel, M.A. Friedl, F.W. Davis, and R.C. Dubayah, 1994. Regression tree analysis of satellite and terrain data to guide vegetation sampling and surveys, *Journal of Vegetation Science*, 5:673-686.
- Mollard, D.G., and J.D. Mollard, 1981. *Heaven Lake Area (NTS 52H/SW), District of Thunder Bay; Ontario Geological Survey, Northern Ontario Engineering Geology Terrain Study 41* (accompanied by Map 5051, Scale 1:100,000), Ministry of Natural Resources, Toronto, Canada, 26 p.
- Moore, I.D., R.B. Grayson, and A.R. Ladson, 1991. Digital terrain modeling: a review of hydrological, geomorphological and biological applications, *Hydrological Processes*, 5:3-30.
- Musick, H.B., and H.D. Grover, 1990. Image textural measures as indices of landscape pattern, *Quantitative Methods in Landscape Ecology, The Analysis and Interpretation of Landscape Heterogeneity*, (M. G. Turner and R.H. Gardner, editors), Ecological Studies Series, Vol 82, Springer-Verlag, New York, pp. 77-103.
- PCI Inc., 1997. *EASI/PACE Image Analysis System Manual, Version 6.0*, PCI Inc., Toronto, Ontario, Canada, variously paged.
- Peddle, D.R., and S.E. Franklin, 1991. Image texture processing and data integration for surface pattern discrimination, *Photogrammetric Engineering & Remote Sensing*, 57(4):413-420.
- Pultz, T.J., and R.J. Brown, 1987. SAR image classification of agricultural targets using first- and second-order statistics, *Canadian Journal of Remote Sensing*, 13(2):85-91.
- Racey, G.D., T.S. Whitfield, and R.A. Sims, 1989. *Northwestern Ontario Forest Ecosystem Interpretations*, NWOFTDU Technical Report No. 46, Ontario Ministry of Natural Resources, Thunder Bay, Ontario, Canada, 160 p.
- Robinson, G.J., 1994. The accuracy of digital elevation models derived from digitised contour data, *Photogrammetric Record*, 14(83):805-814.
- Rosenfield, G.H., and K. Fitzpatrick-Lins, 1986. A coefficient of agreement as a measure of thematic classification accuracy, *Photogrammetric Engineering & Remote Sensing*, 52(2):223-227.
- Rotunno, O.C., P.M. Treitz, E.D. Soulis, P.J. Howarth, and N. Kouwen, 1996. Texture processing of synthetic aperture radar data using second-order spatial statistics, *Computers and Geosciences*, 22(1):27-34.
- Rowe, J.S., 1972. *Forest Regions of Canada*, Publication No. 1300, Canadian Forestry Service, Department of the Environment, Ottawa, Ontario, Canada, 172 p.
- Shepherd, P.R., 1994. Airborne remote Sensing Data, *Rinker Lake Data Report - 1993-1994*, (V.J. Kalnins, P.M. Treitz, and P.J. Howarth, editors), Technical Report ISTS-EOL-TR94-002, Earth-Observations Laboratory, Waterloo, Ontario, pp. 3-19-3-48.
- Shepherd P.R., J.R. Freemantle, S. McArdle, and J.R. Miller, 1995. A comparison of different operational reflectance generation methods applied to airborne CASI imagery, *17th Canadian Symposium on Remote Sensing: Radar Remote Sensing: A Tool for Real-Time Land Cover Monitoring and GIS Integration*, 13-15 June, Saskatoon, Saskatchewan, pp. 268-273.
- Sims, R.A., W.D. Towill, K.A. Baldwin, and G.M. Wickware, 1989. *Field Guide to the Forest Ecosystem Classification for Northwestern Ontario*. Ontario Ministry of Natural Resources, Toronto, Ontario, 191 p.
- Sims, R.A., and P. Uhlig, 1992. The current status of forest site classification in Ontario, *Forestry Chronicle*, 68(1):64-77.
- Sims, R.A., B.G. Mackey, and K.A. Baldwin, 1995. Stand and landscape level applications of a forest ecosystem classification for northwestern Ontario, Canada, *Annales des Sciences Forestiere*, 52:573-588.
- Strahler, A.H., C.E. Woodcock, and J.A. Smith, 1986. On the nature of models in remote sensing, *Remote Sensing of Environment*, 20:121-139.
- Swain, P.H., and S.M. Davis, 1978. *Remote Sensing: The Quantitative Approach*, McGraw Hill, Inc., Toronto, Ontario, 396 p.
- SYSTAT Inc., 1992. *SYSTAT User's Guide - Statistics*, SYSTAT Inc., Evanston, Illinois, 724 p.
- Tom, C.H., and L.D. Miller, 1984. An automated land-use mapping comparison of the Bayesian maximum likelihood and linear discriminant analysis algorithms, *Photogrammetric Engineering & Remote Sensing*, 50(2):193-207.
- Treitz, P.M., 1997. *Boreal Forest Ecosystem Characterization at Site and Landscape Scales using Multispatial Resolution Remote Sensing Data*, PhD thesis, Department of Geography, University of Waterloo, Waterloo, Ontario, Canada, 297 p.
- Treitz, P.M., P.R. Shepherd, P.J. Howarth, and J.R. Miller, 1996. Integrating remote sensing data and terrain variables to discriminate forest ecosystems in northwestern Ontario, *26th International Symposium on Remote Sensing of Environment / 18th Canadian Symposium on Remote Sensing*, Vancouver, B.C., 25-29 March, pp. 515-518.
- Ulaby, F.T., F. Kouyate, B. Brisco, and T.H.L. Williams, 1986. Textural information in SAR images, *IEEE Transactions on Geoscience and Remote Sensing*, 24(2):235-245.
- Vickers, A.L., and J.W. Modestino, 1982. A maximum likelihood approach to texture classification, *IEEE Transactions on Pattern Analysis and Machine Intelligence*, 4(1):61-68.
- Vogelmann, J.E., T. Sohl, and S.M. Howard, 1998. Regional characterization of land cover using multiple sources of data, *Photogrammetric Engineering & Remote Sensing*, 64(1):45-57.
- Walsh, S.A., R. Sims, and J. Ford, 1994. General description of the Rinker Lake Research Area, *Rinker Lake Data Report - 1993*, (V.J. Kalnins, P.M. Treitz, and P.J. Howarth, editors), Technical Report ISTS-EOL-TR94-002, Earth-Observations Laboratory, Waterloo, Ontario, pp. 2-5-2-14.
- Wilson, B.A., 1996. Estimating coniferous forest structure using SAR texture and tone, *Canadian Journal of Remote Sensing*, 22(4):382-389.
- Wulder, M.A., E.F. LeDrew, S. Franklin, and M. Lavigne, 1998. Aerial image texture information in the estimation of northern deciduous and mixed wood forest leaf area index (LAI), *Remote Sensing of Environment*, 64:64-76.
- Yuan, X., D. King, and J. Vlcek, 1991. Sugar Maple decline assessment based on spectral and textural analysis of multispectral aerial videography, *Remote Sensing of Environment*, 37:47-54.

(Received 25 August 1998; revised and accepted 26 March 1999)